sciendo

ARTIFICIAL SATELLITES, Vol. 57, No. 1 – 2022
DOI: 10.2478/arsa-2022-0003

QHY-174M-GPS CAMERA AS THE DEVICE FOR PHOTOMETRY OF ARTIFICIAL SATELLITES

Viktor KUDAK, Vasyl PERIG

Uzhhorod National University, Space Research Laboratory, Uzhhorod, Ukraine

e-mails: viktor.kudak@uzhnu.edu.ua, vasyl.perig@uzhnu.edu.ua

ABSTRACT. In this paper, we make an attempt to use the QHY174M-GPS camera for the photometry research of fast-rotating artificial objects including debris, satellites and rocket bodies. This device is useful for imaging occultations, eclipses, meteors, and so on due to a highly precise recording of the time (GPS-based) and location of the observation on every frame and fast readout of the CMOS detector. The precision of time registration by the QHY174M-GPS camera is at the level of microseconds. All light curves obtained by studied camera during observations of artificial satellites in this work were carried out at Derenivka Observatory of Uzhhorod National University, Ukraine. The created photometric system with QHY174M-GPS camera as the detector and reflector telescope with parameters D=120 mm, F=114 mm, FOV=2.82°×1.76° was calibrated. For target observations, SharpCap software was used. For the purposes of photometry processing, `ccd_phot` software was developed using Python 3.8 programming language with astropy and photutils packages. Photometry observations of artificial satellites of the Earth and standard stars were carried out. Over 80 lightcurves of artificial satellites were obtained. Comparing synchronous observations from two sites, separated 15 km from each other, we can conclude that photometry on the QHY174M-GPS camera gave us the same shape of lightcurve and additional advantages, such as time of exposure or simplicity of usage.

Keywords: instrumentation: detectors, methods: data analysis, techniques: image processing, techniques: photometric, artificial satellites of Earth.

1. INTRODUCTION

In this research, we use QHY174M-GPS COLDMOS camera with GPS-based precision time that can provide exposure time with an accuracy at the level of 10^{-6} s and function of location determination. According to Salazar Manzano et al. (2019), the camera has short dead time between frames $\sim$ 20 ms. The QHY174M-GPS camera has dual-stage thermoelectric cooling to -45°C below ambient temperature with full anti-moisture control including a heated optical window. The camera can be equipped with a 4-pin QHYCFW2 filter wheel control port or optical filter tight before CCD chip. We did not use the filter wheel. For LEO satellite photometry, filter change should be very fast, so we prefer one filter installed in the front of the camera. Camera also has an anti-amp glow function and can reduce the IMX174 sensor's amplifier glow significantly in long exposures. Specifications of the QHY174M-GPS camera are listed in Tab.1 and general view of the camera with GPS antenna presented in Figure 1.

The properties of QHY174M-GPS camera are useful for imaging occultations, eclipses, meteors, and other scientific imaging requiring a highly precise recording of the time and location of the observation on every frame (e.g. Gault et al., 2020; Salazar Manzano et al., 2019). In the work of Kaminski et al. (2018), the authors use QHY174M-GPS camera for astrometry of artificial satellites. Also Zolnowski et al. (2019) compare this camera to dynamic vision sensor (DVS) event cameras, where they show that QHY camera has about 1.6 mag better limiting magnitude and better timing resolution compared to the DVS camera. Such properties are also suitable for artificial satellites photometry studies. In this paper, we will explore the possibility and advantages of QHY174M-GPS camera usage for photometry of artificial satellites of the Earth.

Figure 1. QHY-174M GPS CMOS camera (left) and view of the camera with GPS antenna (right)

All light curves (LC) obtained during observations of artificial satellites in this work were carried out at Derenivka Observatory of Uzhhorod National University, Ukraine (Lat: 48.563417 N; Long: 22.453758 E). For our observation, we used a refractor telescope with a diameter of 120 mm and an equivalent focus of 114 mm. The telescope was mounted as the additional device on the alt-azimuth mount of TPL-1M (1 meter class) telescope that can be operated from PC. QHY174M-GPS camera was used with Johnson R photometric filter. The field of view of such system configuration is $2.82° \times 1.76°$, with scale 10.6 arcsec/pixel.

Frame capturing was performed by SharpCap[1] software, a powerful astronomy camera capture tool. This software is currently the only solution that can handle frame grabbing with use of internal camera storage that is necessary if we are dealing with small exposures, with this approach we can achieve declared small times of exposures and write GPS-based time in FITS header. The camera was usually used in 2×2 binning mode (960×600 pixels).

[1] https://www.sharpcap.co.uk/

Table 1. QHY-174M GPS CMOS camera characteristics

Model	QHY174GPS M
Sensor	SONY IMX174 CMOS
Pixel Size	5.86 µm ×5.86 µm
Effective Pixel Area	1920×1200
Effective Image Area	11.25mm×7.03mm
QE	78%
AD Sample Depth	12/10bit (output as 16bit and 8bit)
Frame Rate	138FPS@1936×1216, 260FPS@960×600
Readout Noise	5.3e-@Gain0% 2.8e-@Gain60% 1.6e-@Gain100%
Exposure Time Range	from 5 µs to 900 sec
Binning	1×1, 2×2
Anti-Glow Control	Yes (Reduces amplifier glow significantly)
Shutter Type	Electric Global Shutter
Computer Interface	USB 3.0 Super Speed
Cooling System	Dual Stage TEC cooler (-40C below ambient)
Time-Stamp Precision	1 micro-second of the GPS UTC clock

2. CALIBRATION OF THE PHOTOMETRY SYSTEM

The calibration of the photometric system must be made to evaluate standard magnitude values based on the flux registered by the camera. This process involves the definition of system zero point and coefficient of transformation to the selected standard bandwidth (Johnson R in our case). To calibrate our photometric system, we use Landolt standard stars studied in Landolt (1992).

To automatically process frames with calibration stars, all FITS files must contain a world coordinate system (WCS) information. After capture by the SharpCap software, FITS files do not contain WCS in the header because SharpCap is not connected with TPL-1M telescope mount. To obtain WCS information, we use astrometry.net (Lang et al. 2010) software that can take any image of stars (where stars are points) without WCS, solve a field and obtain the WCS information that we can later write to the FITS header.

Script for frames processing and calibration `stars_calibr_land.py` is a part of `ccd_phot` project[2]; it is written on Python 3.8, source code available on GitHub. This script uses *astropy*, *photutils* python packages and photometry errors are estimated with procedures used in Wide Field Camera 3 photometric pipeline[3] described in Gennaro et al. (2018).

Before processing, all the available frames was corrected by dark frames and flat fields. Based on the fact that now all frames contain WCS information in our script, we convert known celestial coordinates of star from Landolt catalogue (α, δ) to physical coordinates of the frame (X, Y). To ensure that there are no errors caused by optics distortions or other factors, we perform star centring and profile fitting. As the result, we obtain real coordinates (X_r, Y_r) of star profile centre. In general, differences X-X_r are within 0.2 – 0.5 of a pixel, but this operation is preferable to increase the precision of aperture photometry in the next step.

[2]https://github.com/vkudak/ccd_phot/

[3]https://github.com/spacetelescope/wfc3_photometry

We selected the best method for star profile fitting by fitting different functions and calculating coefficient of determination R^2 that represents the goodness-of-fit. As the tested functions, we use Gauss, Lorentz and Moffat 2D functions. The coefficients of determination R^2 for these functions are given in Tab. 2. According to these data, the best fit is achieved by fitting with Moffat 2D function. These results are in good agreement with Racine (1996) or Devyatkin et al. (2010) where the authors prefer an approximation of the star profile by the Kolmogorov profile function as the superposition of two Moffat functions. We prefer not to use complex Kolmogorov profile function because Moffat function seems to be sufficient for our task of precise star centre definition. The more complex function will only take more time for fitting and will not substantially increase the accuracy. The example of star profile fit with Moffat 2D function and its residuals are presented on Fig. 2 for Landolt star *SA 114 176* ($\alpha = 22:43:11$, $\delta = +00:21:09$, $m_R = 8.44$, $m_V = 9.24$, ***SpType = K4/5 E***); star was registered on the frame with signal-to-noise ratio $\frac{S}{N} \sim 100$.

Table 2. The goodness of star profile fit with different functions

Function	**Gauss**	**Lorentz**	**Moffat**
R^2	0.8623	0.9166	0.9477

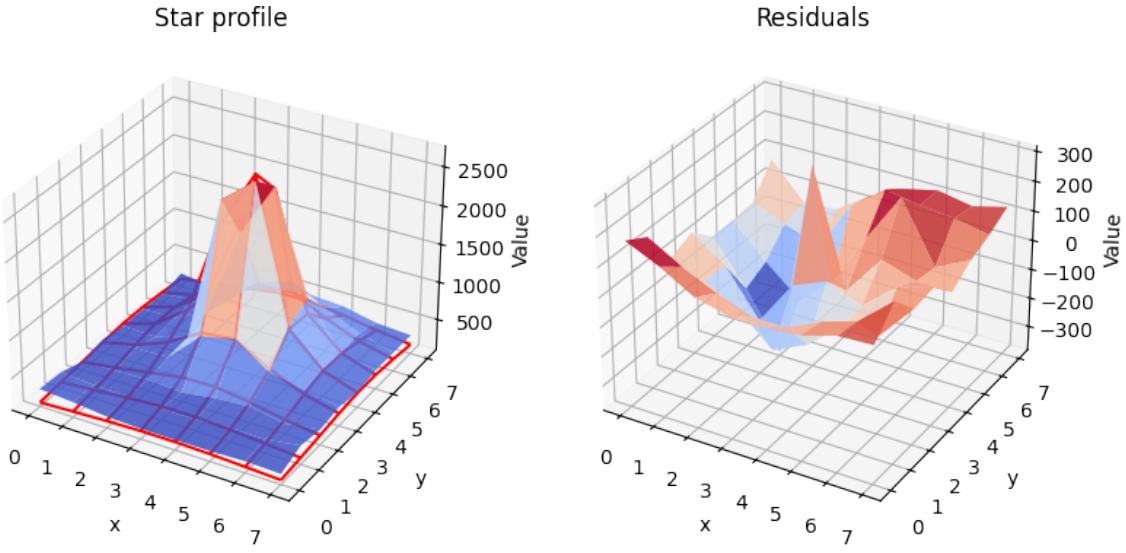

Figure 2. Left: star profile with Moffat 2D function fit (red). Right: Residuals.

For system calibration, we choose four regions from Landolt catalog of standard stars (SA 112, SA 113, SA 114 and SA 115) with 39 stars that have magnitude in R band m_R brighter than 14 mag and elevation $h > 30°$ at the moment of observation. The observation was made with 10-second exposures. The standard stars and their magnitudes and spectral types are listed in Table 3. From each region, we obtain 50 – 70 frames. In our processing script, we calculate an average value of flux (F_R) registered from each star.

Table 3. Selected standard stars from Landolt catalogue

Star Name	m_V	m_R	V-R	SpType	Star Name	m_V	m_R	V-R	SpType
SA 112 275	9.905	9.258	0.647	K2 D	SA 113 366	13.537	12.914	0.623	–
SA 112 595	11.352	10.453	0.899	K2:III D	SA 113 177	13.560	13.104	0.456	–
SA 112 223	11.424	11.151	0.273	F5 D	SA 113 195	13.692	13.274	0.418	–
SA 112 704	11.452	10.630	0.822	–	SA 113 272	13.904	13.534	0.370	–
SA 112 822	11.549	10.991	0.558	G8:III D	SA 113 307	14.214	13.584	0.630	–
SA 112 805	12.086	12.023	0.063	A0 D	SA 113 182	14.370	13.968	0.402	–
SA 112 250	12.095	11.778	0.317	F8 D	SA 114 176	9.239	8.439	0.800	K4/5 E
SA 113 466	10.004	9.723	0.281	F5 D	SA 114 670	11.101	10.456	0.645	K1.5:III D
SA 113 475	10.306	9.736	0.570	G5 D	SA 114 548	11.601	10.863	0.738	K2 D
SA 113 342	10.878	10.341	0.537	–	SA 114 654	11.833	11.465	0.368	G0 D
SA 113 156	11.224	10.921	0.303	–	SA 114 750	11.916	11.889	0.027	B9 D
SA 113 259	11.742	11.121	0.621	K0:III D	SA 114 446	12.064	11.667	0.397	–
SA 113 493	11.767	11.337	0.430	G5 D	SA 114 656	12.644	12.097	0.547	K1:III D
SA 113 440	11.796	11.433	0.363	–	SA 115 271	9.695	9.342	0.353	F8 D
SA 113 459	12.125	11.818	0.307	–	SA 115 516	10.434	9.871	0.563	G8IV D
SA 113 492	12.174	11.832	0.342	G0 E	SA 115 420	11.161	10.875	0.286	F5 D
SA 113 339	12.250	11.910	0.340	F8 D	SA 115 554	11.812	11.226	0.586	K1.5:III C
SA 113 191	12.337	11.866	0.471	–	SA 115 412	12.209	11.882	0.327	–
SA 113 495	12.437	11.925	0.512	G: D	SA 115 268	12.494	12.128	0.366	–
SA 113 158	13.116	12.709	0.407	–					

As the result, we can write a system of equations (1) that can be solved with the least-squares method as shown in Kudak et al. (2017a).

$$\begin{cases} A + c_R(V-R)_1 = m_R + 2.5\log(F_R/T_{\text{exp}})_1 + k_R(M_z)_1 \\ A + c_R(V-R)_2 = m_R + 2.5\log(F_R/T_{\text{exp}})_2 + k_R(M_z)_2 \\ \qquad\qquad \cdots \\ A + c_R(V-R)_i = m_R + 2.5\log(F_R/T_{\text{exp}})_i + k_R(M_z)_i \end{cases} \tag{1}$$

where A is a zero point of photometric system, c_R the coefficient of transformation into the corresponding band of standard photometric system (Johnson R), F_R the flux obtained in R band, T_{exp} the time of exposure, M_z the airmass at zenith angle z, k_R the coefficient of extinction for R band that we define equal to 0.16. Our k_R value is in good agreement with Miller et al. (1996) and Sanchez et al. (2007).

From this system, we can calculate zero point of the photometric system A and coefficient of transformation to standard R band c_R. These values are $A = 18.6725 \pm 0.0764$ and $c_R = -0.0141 \pm 0.0008$.

3. PHOTOMETRY OF ARTIFICIAL SATELLITES

In Space Research Laboratory (SRL) of Uzhhorod National University, we are dealing with photometry of artificial satellites for almost 40 years. We have a huge experience and catalogue of LC corresponding to hundreds of satellites. We started to obtain photometry LC of artificial satellites in 1970 with use of electro-multipliers (see Bratiichuk et al., 1979). The photometry observations continued in year 2000 with the installation of laser ranging telescope TPL-1M. This telescope was reconstructed to a photometry system with electro-multiplier (see e.g. Kudak et al., 2017a, Kudak et al., 2017b, Epishev et al., 2018).

The photometric system with electro-multiplier is obsolete and comes with many disadvantages compared with new CMOS devices. To achieve good photometry data, we decide to switch to CMOS photometry. A new optical system with QHY174 camera, described above in this paper, is a prototype system that we made to see if we can obtain LC of LEO satellites in good quality. Our goal was to try to use new CMOS camera and develop software that can be used to obtain light curves of artificial satellites.

For our purposes, we select mainly bright satellites up to $5-7$ standard magnitude with a rotation period between $5-10$ seconds. The period restrictions are due to minimal exposure time limitation ($0.2-0.5$ s) caused by small aperture and the necessity to obtain at least 10-20 points at the period interval. Another criterion was a visual speed of satellite that should be up to $1°$/s to ensure that mount will be able to track the target.

In this section, we will briefly describe the process of photometry processing and present the results of photometry obtained by the QHY174M-GPS camera.

The tracking of selected for photometry observations artificial satellites was performed by software developed for TPL-1M mount according to ephemeris computed from two-line elements (TLE). The mount can track satellites with speed up to 1.2 °/s. SharpCap software can save each capture session in a different directory according to the time of capture start and name of the target. This feature is very useful and when we need to process the frames that correspond to individual satellite pass and obtain a light curve, we can process FITS files in an appropriate directory that correspond to that pass.

Script for processing satellite passes (`sat_phot.py`) is a part of `ccd_phot` project. As input parameter for `sat_phot.py` script, only the path to FITS files must be passed. Additional information as (I) name of a satellite (NORAD, COSPAR or just NAME), (II) a path to file where two-line elements (TLE) are available for this satellite, (III) zero point of the system (A), (IV) the extinction coefficient (k), (V) the window size for target search (gate), and (VI) aperture and annuals radii (r_{ap}, r_in, r_out) are read from a configuration file that must be present in the same directory where FITS files are located.

In the header of the first FITS file, the position of the target must be specified (OBJX, OBJY keywords in FITS header). By reading this information, our script will get the initial data to know where to look for a target in the frame. Without defining the initial position of the target, the script cannot perform photometry because it is difficult to define the difference between star/hot pixel and satellite, even if stars are tracks on the frame. An example of the frames that are processed by our software shown in Fig. 3.

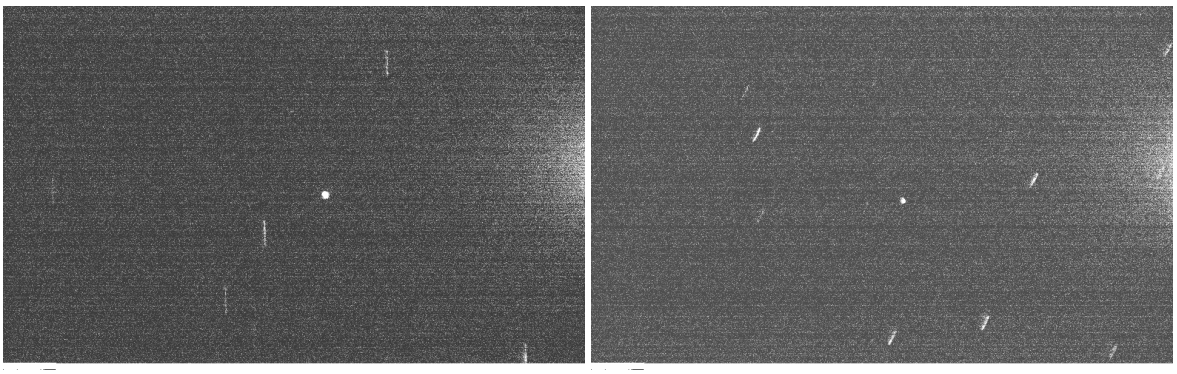

Figure 3. Example of FITS files to process. Object is in the centre of the frame and its shape is point, the stars have trail shape.

As the next step in the script, we perform centring of the target according to the brightest pixel in the window (size defined in the config file) with centre in (OBJX, OBJY) pixel and 2D Moffat fitting to define the precise position of target centre as described in the previous section and then perform aperture photometry at this position.

After we measure the flux at the defined position of target centre, the script also calculates additional parameters as air mass, elevation, range to satellite according to available TLE. Operating with such data, we can calculate instrumental magnitude (m_{inst}) and standard magnitude (m_{st}) according to equations:

$$m_{\text{inst}} = -2.5 \cdot \log(F/T_{\text{exp}}) \tag{2}$$

$$m_{\text{st}} = A + m_{\text{inst}} + m_z + m_r \tag{3}$$

where F is a registered flux, T_{exp} the time of exposure, A a system zero point calculated in section 2, m_z and m_r the corrections for air mass and correction for standard range that is defined as 1000 km for a case of artificial satellites and m_z, m_r are defined by equations:

$$\begin{aligned} m_z &= k \cdot \frac{1}{cos(z)} \\ m_r &= -5 \cdot \log \frac{R}{1000} \end{aligned} \tag{4}$$

where z is a zenith angle of the satellite, k is the coefficient of extinction nad R is the distance from the observer to the satellite.

A logical diagram of `sat_phot.py` script is presented in Fig. 4. As the result of script execution, we obtain a file with fluxes, standard magnitudes in R filter, the errors, azimuth, elevation and distance to the satellite at each moment of observation. This file can be interpreted as a light curve. Example of processed LC is presented in Fig. 5.

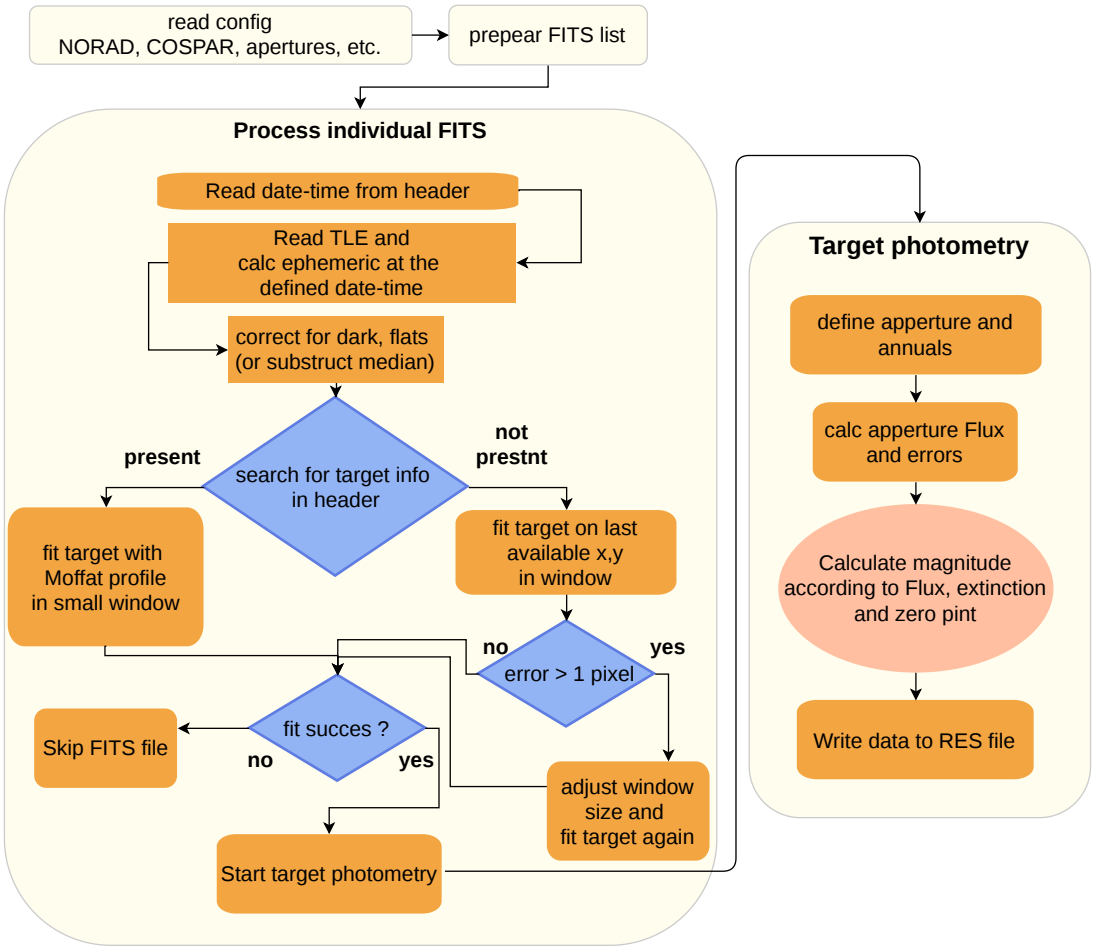

Figure 4. Logical diagram of the satellite photometry script

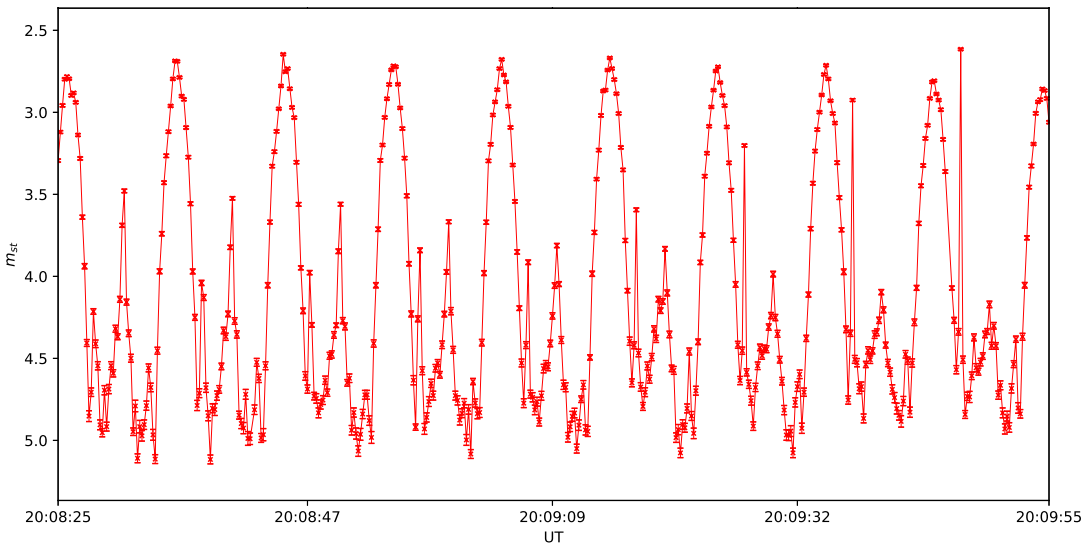

Figure 5. Part of LC of Topex/Poseidon artificial satellite (NORAD 22076) observed at Derenivka station on Aug 06 2020 in R filter. Time of exposition 0.2 sec. Photometry errors are $0.006 \div 0.040$ mag.

Thus, we obtain more than 80 LCs. To compare the shape of satellite's light curve, we observe it from two observational points, Uzhhorod and Derenivka, which are 15 km apart from each other. In Uzhhorod (Lat: 48.631639 N; Long: 22.299167 E, reflector with D=100 mm, F=1000 mm), we obtain LC in B and V filters with photo-multiplier as a light detector (time of exposition 0.5 sec), time was synchronized from GPS. Meanwhile, in Derenivna, we obtain LC in R filter with QHY174M-GPS camera (time of exposition 0.3 s). Lightcurves in BVR filters of satellite NORAD 40358 observed in such way are depicted in Fig. 6. Also colour indexes are presented at the bottom part of same figure.

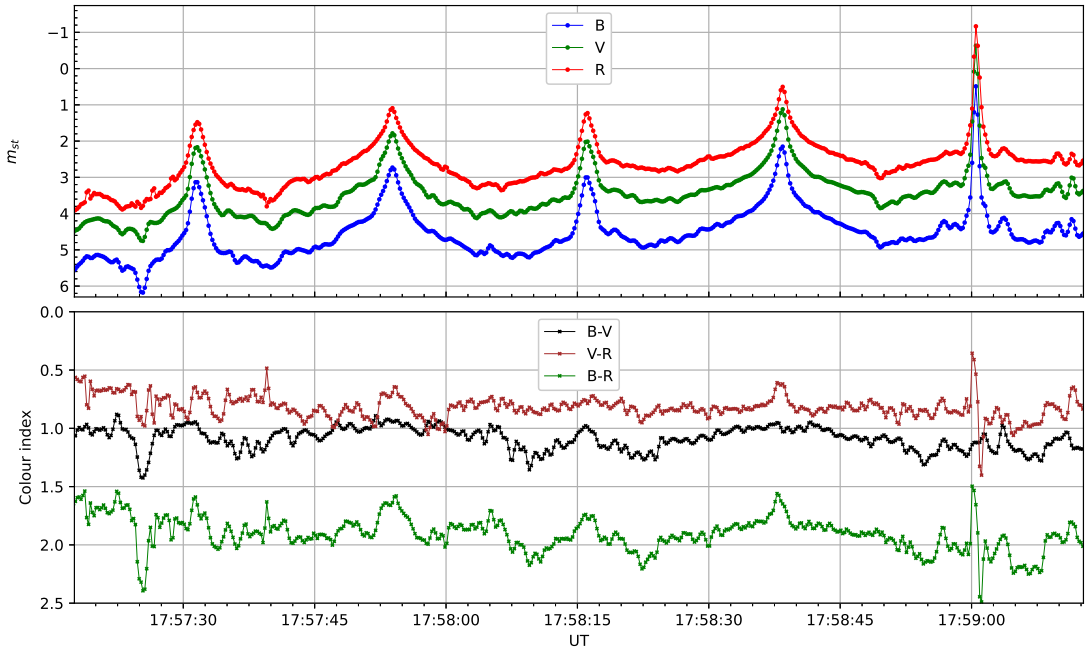

Figure 6. Top: Observations of satellite COSMOS 2502 (NORAD 40358) from two observational sites - Uzhhoorod in B,V filters with use of photo-multiplier (blue and green lines), Derenivka in R filter with QHY174M-GPS camera (red line). Observation made on Nov 09 2020. Bottom: Colour indexes B-V, V-R and B-R

4. CONCLUSIONS

Our study has shown that QHY174M-GPS camera is an excellent tool for photometric observations of fast-rotating space objects. The key advantages of this camera include the fallowing: precise time registration; low latency between frames; short exposures and physical form factor. The only disadvantage that we can mention is the fact that observation must be made only using SharpCap software. When using a camera with small exposures ($\sim 0.1-0.001$ s), we face the problem of light lack. To solve this problem, we suggest to use a telescope with a small focal ratio ($F/D \sim 1-1.5$).

To process photometry frames, `ccd_phot` software was written. Scripts included in this package also allow the user to calibrate photometry system based on the Landolt standard stars. The software uses aperture photometry approach for the photometry of satellites and for calibration by standard Landolt stars. Maybe in the future, we will also try to implement PSF photometry for these tasks.

The calibration of our photometry system gave us the following values of system zero point and coefficient of transformation: $A = 18.6725 \pm 0.0764$ and $c_R = -0.0141 \pm 0.0008$, respectively.

The coefficient of transformation value is close to zero, which means that our photometric system's effective wavelength is close to the effective wavelength of the standard Johnson R passband.

We also made a comparison of light curves of the same satellite (NORAD 40358) observed synchronously from two different observatories. Unfortunately, due to that fact that we do not have two same filters, we did not use the same filter in two photometric systems to perform full LC comparison. In Uzhhorod, we obtained light curves in B and V Johnson filters. In Derenivka we used R Johnson filter. According to the shape of the LCs, we are fully satisfied with the result of photometry by the QHY174M-GPS camera. Analysing colour indexes, we can say that they are almost the same on the whole LC with exception at the end of the LC where we can observe satellite's spike (UT $\sim$ 17:59:00). This spike has almost the same magnitude in V and R bands.

Acknowledgements. The research was partialy supported from Ukrainian National grand № 0119U100236.

REFERENCES

Bratiichuk, M. V., Epishev, V. P., & Motrunich, I. M. (1980) Study of the surface shape of Pageos from photoelectric observations, *Astrometriia i Astrofizika*, Vol. 40, 78-89.

Devyatkin A. V., Gorshanov D. L., Kouprianov V. V., et al. (2010) Apex I and Apex II software packages for the reduction of astronomical CCD observations, *Solar System Research*, Vol. 44, No. 1, 68-80.

Epishev, V. P., Kudak, V. I., Perig, V. M., Motrunich, I. I., Naybauer, I. F., Novak, E. J., & But, O. Y. (2018) Influence of the Gravitational Fields of the Moon and the Sun on Long-Period Variations in the Proper Rotation of "Midas" Satellites, *Astrophysical Bulletin*, Vol. 73 No.3, 363-372.

Gault D., Barry T., Nosworthy P., .et al. (2020) A New Double Star from an Asteroid Occultation TYC 6356-00058-1, *Journal of Double Star Observations*, Vol. 16, No. 5, 440-443.

Gennaro, M., Anderson, J., & Baggett, S. (2018) WFC3 Data Handbook, Version 4.0. *STScI*, Baltimore, MD.

Kaminski K., Wnuk E., Golebiewska J., et al. (2018) LEO cubesats tracking with a network of Polish optical SST sensors, *In Proceedings of the AMOS conference.*

Kudak V. I., Epishev V. P., Perig V. M. et al. (2017 a) Determining the orientation and spin period of TOPEX/Poseidon satellite by a photometric method, *Astrophysical Bulletin*, Vol. 72, No. 3, 340-348.

Kudak V.I., Perig V.M., Neubauer I.F. (2017 b) Studying of the own rotation period changes of satellite "Ajisai" on the interval 1986-2017, *Uzhhorod University Scientific Herald. Series Physics*, Vol. 41, 140–145.

Landolt A. U. (1992) UBVRI Photometric Standard Stars in the Magnitude Range 11.5<V<16.0 Around the Celestial Equator, *Astronomical Journal*, Vol. 104, 340.

Lang D., Hogg D. W., Mierle K., et al. (2010) Astrometry. net: Blind astrometric calibration of arbitrary astronomical images, *The Astronomical Journal*, Vol. 139, No.5, 1782.

Miller R., & Osborn W. (1996) All-Sky UBVRI Photometry with a Celestron-14, *International Amateur-Professional Photoelectric Photometry Communications*, Vol. 63, 40.

Racine R. (1996) The Telescope Point Spread Function, *PASP*, Vol. 108, No. 726, 699

Salazar Manzano L.E, Ángel Parra Patiño M., Ángel Salazar Manzano M., et al. (2019) Analysis of synchronism and response velocity in instrumental assemblies for the observation of stellar occultations, *Journal of Physics: Conference Series*, Vol. 1247, No.1, 012041

Sánchez S. F., Aceituno J., Thiele U., et al. (2007) The Night Sky at the Calar Alto Observatory, *PASP*, Vol. 119, No. 860, 1186

Żołnowski M., Reszelewski R., Moeys D. P., et al. (2019) Observational Evaluation of Event Cameras Performance in Optical Space Surveillance, *Proc. 1st NEO and Debris Detection Conference, Darmstadt, Germany, 22-24 January 2019*.

Received: *2021-04-14*

Reviewed: *2021-07-09 (undisclosed name); 2021-07-25 (undisclosed name);*
2021-01-04 (V. Reddy)

Accepted: *2022-01-31*